atmosphere

MDPI

Review

AI/ML-Enhanced Wind Forecasts for Reducing Uncertainty in Prescribed Fire Planning

Sara Brambilla *, Shane Xavier Coffing, Jesse Edward Slaten, Diego Rojas, David Joseph Robinson and Arvind Thanam Mohan

Los Alamos National Laboratory, Bikini Atoll Rd., Los Alamos, NM 87545, USA; jslaten@lanl.gov (J.E.S.); drobinson@lanl.gov (D.J.R.); arvindm@lanl.gov (A.T.M.)

* Correspondence: sbrambilla@lanl.gov

Abstract

Prescribed fire is a vital tool for ecosystem management and wildfire risk reduction but its escalation is constrained by overly conservative burn windows because of uncertainties, for instance, in wind forecasts. This review describes the state of the art in weather product use by fire/smoke models and identifies three priority research gaps that artificial intelligence/machine learning (AI/ML) is well positioned to address: (1) spatial and temporal downscaling to meter-scale, sub-hourly wind fields; (2) bias correction for systematic model errors in complex terrain; and (3) robust uncertainty quantification to inform ensemble-based simulations. Emerging AI/ML techniques offer promising frameworks to address all three challenges. By providing high-resolution, bias-corrected, and probabilistic wind fields, AI/ML-enhanced forecasts will allow for expanded burn windows, improved ignition strategy design and a reduced reliance on expert intuition, especially when a prescribed fire is introduced into new areas.

Keywords: prescribed fire; burn window; wind forecasting; AI/ML opportunities; next-generation fire models

1. Introduction

The first widely adopted wildfire model was developed in 1972 by Rothermel [1]. The model's ability to quickly provide actionable answers in moments of crisis paved the way for its diffusion across the wildland fire community. In recent years there has been a growing interest in developing modeling capabilities to capture a different type of wildland fire: prescribed fire, where fuel is intentionally ignited to reach predefined risk management objectives to increase human safety, protect infrastructure, and reduce the consequences of following wildfires through fuel load reduction. Simultaneously, prescribed fire serves as an ecosystem management tool to control for invasive species, insects, and diseases, to perpetuate fire-dependent species, and to maintain biodiversity [2]. Prescribed fires are ignited to consume surface and/or understory fuel while avoiding tree mortality. Less often, prescribed fires are intentionally of high intensity, especially in ecosystems where fire is naturally stand replacing (stand replacing: fire that kills all or most of the living overstory trees in a forest and initiates forest succession or regrowth [3]). Prescribed fire planning considers the fire environment, i.e., the set of conditions that affect fire behavior given a chosen ignition strategy (see Figure 1) and it includes static aspects, like topography, and dynamic factors, such as fuel moisture and weather. These dynamic conditions and

Academic Editor: Alan Robins

Received: 23 February 2026
Revised: 15 March 2026
Accepted: 16 March 2026
Published: 18 March 2026

their uncertainties must be forecasted in order to select the most appropriate ignition pattern and devise contingency plans.

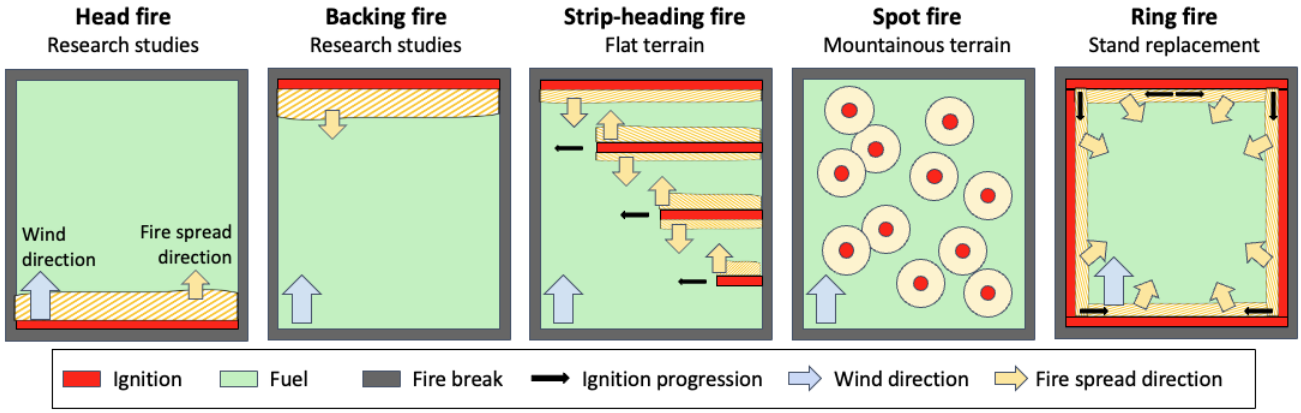

Figure 1. Typical ignition patterns used in prescribed fire operations.

Land and fire managers face growing demands to increase prescribed fire use [4], but their opportunities are limited by the availability of days falling within the "burn window", i.e., fuel and weather conditions under which practitioners are confident that a burn can be conducted effectively and safely (see example in Figure A1). The acceptable conditions defined by the burn window depend heavily on the ability to forecast winds at the burn site and predict how fire and smoke will respond. Uncertainty in the forecast can lead to overly conservative evaluations, which unnecessarily constrain opportunities, meaning that some burns will not be conducted in a certain year and will have to be postponed until the following year, when the cycle repeats. Expanded prescribed fire use, as proposed in [4], can only be achieved by expanding the burn windows, avoiding over conservatism, while assuring that fires can be performed in a safe manner and that contingency plans can be adequately developed. This activity cannot rely uniquely on fire managers' expertise, especially when prescribed fire is introduced into a new landscape, and can be supported by the science-informed quantitative characterization of the fire environment.

To answer this call, Hiers et al. [4] brought forward the necessity to develop next-generation fire models to surpass the inability of wildfire models to capture the characteristics of prescribed fire operations. While wildfires occur in extreme conditions of drought and high winds, prescribed fires are ignited in marginal conditions, when fuel moisture is higher and winds are lower, such that the burn consumes the desired amounts and types of fuel without risking spotting and escape. This makes prescribed fire more sensitive than wildfires to local horizontal and vertical heterogeneities in fuels. It is not just fire that is sensitive to these heterogeneities, the wind driving the fire is affected as fuel distribution determines the in-stand wind speed reduction in presence of foliage, and the acceleration in gaps between and below the trees [5]. But fire and winds are not independent actors; their interplay and feedback are what controls the phenomenology [6,7]. This means that next-generation prescribed fire models will have to capture coupled fire–atmosphere interactions and 3D fuel structure to connect site and condition specific ignition patterns with fire and smoke behavior. In particular, Hiers et al. [4] identified the following areas for improvement in support of next-generation fire models:

1. The 3D spatial representation of vegetation structure and its change over time.
2. Ecological fire effects' characterization and their cumulative impact on the ecosystem.
3. Short-term (days) weather forecasting for burn and smoke management planning and long-term (months) climate forecasting for burn plot prioritization.

The focus of this paper is the third area identified above, i.e., next-generation prescribed fire modeling needs in regard to winds. Since the scope of the paper kickstarts the conversation between atmospheric scientists, fire managers, and artificial intelligence/machine learning (AI/ML) developers, we will begin by describing prescribed fire operations and wind products currently used (Section 2). Following this, we will present current challenges and gaps (Section 3) and then discuss how AI/ML can address them, accelerating advancements in meteorology applied to prescribed fire (Section 4).

2. Current Representation of Winds

The three time horizons for planning prescribed fires are landscape-scale long-term plot prioritization, near-future planning, and day of the burn go/no-go decision (Figure 2). The weather products used over those time horizons are discussed in this section.

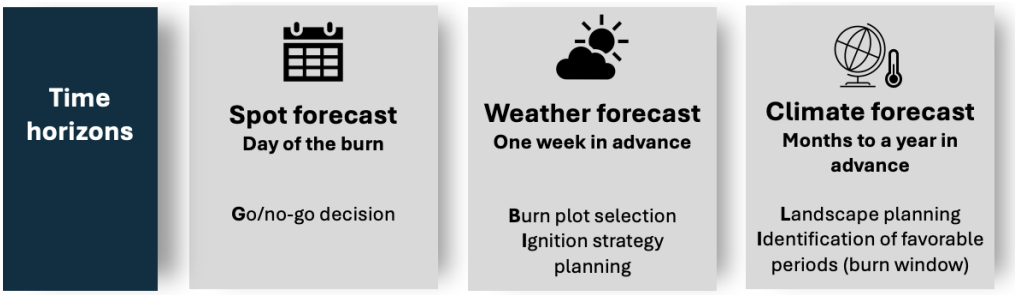

Figure 2. Time horizons over which different planning activities regarding prescribed fires occur.

2.1. Climate Forecasts: Months to Years in Advance

Inter-year climate variability has both direct and indirect effects on winds (Figure 3). Winds are affected directly by changes in atmospheric circulations at the global and local scales. Indirectly, winds are impacted by changes in the forest structure due to disturbances (droughts, diseases, etc.), post-disturbance feedback, where the increase in wind in the forest thinned by disturbances escalates soil drying and trees blowdown (tree blowdown includes both windthrow and windsnap; windthrow refers to tree's uprooting by wind and windsnap refers to the breaking off of the trunk), and ecosystem shifts, where new species move into an area.

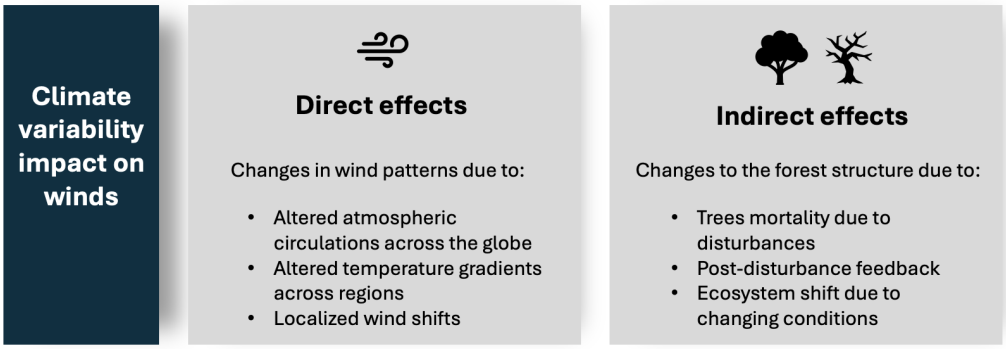

Figure 3. Summary of the effects of climate variability on winds.

The climate forecasts used by fire practitioners are the seasonal outlooks which report the monthly variability from a mean state for the following 12 months. This type of analysis does not identify on which days it will be favorable to burn but rather the period(s) in which relevant weather variables will likely be within the burn window for the geographic area of interest. The scope is understanding the year-to-year changes in the burn season (shortening vs. lengthening vs. shifting) to establish which areas of a landscape can be burned in a certain year.

Studies including the effect of climate change have shown that burn windows may shorten in some parts of the globe [8] but not in others [9] or that the burn season may shift. For the south-eastern U.S., Kupfer et al. [8] predicted that the frequency of suitable burning days will decrease from 65% to 22–41% depending on the emission scenario considered, but no corresponding trend was found for the south-eastern Australia [9], where suitable days may increase. It is worth underlining that different studies have used different methodologies to assess how future conditions will impact burn days. Studies differ in several areas: the climate models used, the emission scenario, the method for downscaling the global model output to regional climate, the periods to compare in terms of the present and future burn days, the weather variables and derived indexes used to determine suitable days, their extrapolation at the likely time of burn vs. daily min/max, and the chosen acceptable ranges.

Insect outbreaks and droughts caused by changes in the climate affect wind indirectly and therefore affect fire behavior through the modification of the forest structure. When a tree dies the foliage/needles fall from the canopy to the ground, leading to a reduction in the canopy's bulk density and drag. This, in turn, leads to changes in wind penetration through the canopy that depend on the actual changes in fuel continuity. For insect outbreaks, fuel continuity is a function of the mixture of host and non-host species and the infestation pattern [10]. In terms of fire spread, higher winds in the modified forest will result in higher fire intensities and spread rate. Also, after foliage and needles fall to the ground there is more ground fuel to carry the fire leading to more robust fires than seen in healthy forests [10]. Hence, predicting the ecosystem trajectory due to disturbances is as important as projecting the changing climatology for prescribed fire planning months to years in advance.

2.2. Weather Forecasts: The Week Leading up to a Burn

Fire practitioners classify winds into surface ($\leq$10 m above ground level; AGL) and transport winds (average between 10 m AGL and the top of the planetary boundary layer (the planetary boundary layer, also known as atmospheric boundary layer or mixing layer, is the lowest part of the Earth's atmosphere that is directly influenced by the Earth's surface where there are rapid (turbulent) variations in wind speed, moisture, and temperature). This is an artificial separation due to the simplicity of early models for smoke transport, e.g., VSMOKE [11,12]. However, this concept is still in use by practitioners and therefore is discussed here to provide context in Section 2.2.1. The use of more modern products is discussed in Section 2.2.2.

2.2.1. Surface and Transport Winds

In an intense wildfire, surface winds and their interaction with topography control the rate, intensity, and directionality of fire spread. In prescribed fires, the ignition pattern and the canopy structure will also play a role. In particular, the wind felt by the fire will depend on the canopy and understory foliage density. Therefore, to use surface winds within a prescribed fire model, one must account for the reduction in wind speed. Cionco [13] correlated the above-canopy winds to in-stand winds through an attenuation coefficient (see Table 1). Figure 4 shows the wind speed reduction for a subset of vegetation types: in-stand reduction can be >90% in some cases. This approach captures the vertical profile through the canopy and can be adapted to include the increase in wind speed in areas without foliage (e.g., below the canopy base height in absence of mid-story fuel). This approach is for instance applied in QUIC-Fire [7].

Table 1. Attenuation coefficient [14] to compute the wind speed (u) within the canopy at as $u(z) = u_h exp(\alpha(z/h - 1))$, where z is the height below the canopy, h is vegetation height, and u_h is the wind speed at the vegetation height.

Canopy Type	Attenuation Coefficient (α)	Canopy Type	Attenuation Coefficient (α)
Citrus orchard	0.44	Oak–gum forest	2.68
Larch	1.00	Spruce forest	2.74
Christmas trees	1.06	Immature corn	2.82
Flexible stalks	1.67	Jungle	3.84
Corn	1.97	Maple–fir forest	4.03
Wheat	2.45	Gum–maple forest	4.42

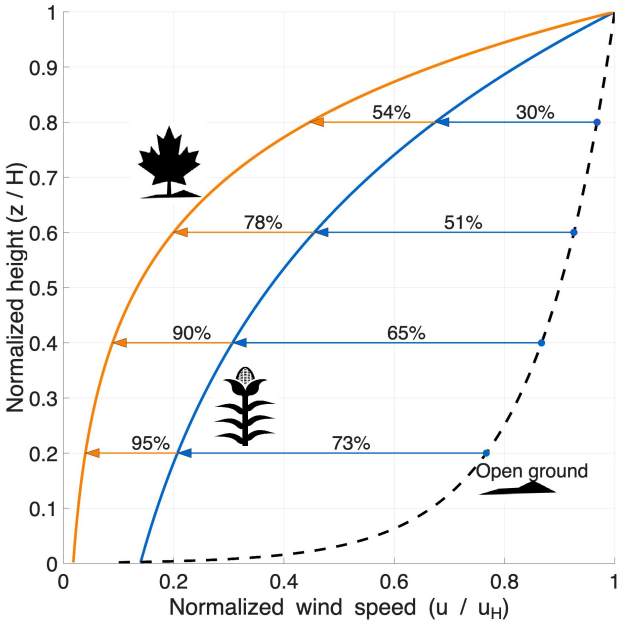

Figure 4. In-stand attenuated wind speeds for a subset of vegetation types. A reduction greater than 90% compared to open ground can be seen for maple–fir forest.

A similar approach was developed by Albini [15], where in-stand mid-flame winds are derived from 6.1 m (20-ft) above-canopy winds through a "wind adjustment factor". A similar concept is that of a "wind reduction factor", which is used to derive winds at 10 m [16]. The main disadvantage of both factors is that they do not capture the vertical wind profile throughout the canopy and the increase in wind speed below the canopy base height. Moon et al. [16] have found that when comparing different vertical locations within the canopy, the reduction factor can change up to a factor of four. The fire model built on top of the Weather Research and Forecasting model (WRF-SFIRE) uses wind adjustment factors [17], and computes them based on the model cell fuel classification. Other rules of thumb used in the prescribed fire community to correlate in-stand to above-canopy or open-area winds can be found in Waldrop and Goodrick [18].

Upper winds are responsible for carrying the smoke away from the burn plot. The wind speed determines the dilution of the smoke plume as its concentration is roughly inversely proportional to wind speed while its lateral and vertical spread is controlled by atmospheric stability and turbulence [19]. In fire applications, very simple smoke models are oftentimes used, such as VSMOKE [11,12]. Given their inability to use a vertical wind profile, a different proxy variable was developed: the transport wind, which is defined as the average from the surface (>10 m AGL) to the height of the boundary layer. For prescribed fires, the fire intensity can vary during the duration of the fire, leading to smoke

being injected at different heights. In the presence of wind direction shear with height, the more positively buoyant smoke may be transported in a different direction than less buoyant smoke. An anecdotal example of wind direction shear with height is shown in Figure 5.

Figure 5. Wind direction shear seen in the meandering path of the smoke from a stack. Photo taken in Salt Lake City on 14 June 2025 by Rod Linn, Los Alamos National Laboratory, which can be reused under the CC BY license [20].

Experimental data [21], numerical simulations [22,23], and theoretical derivations [24] have shown that surface winds typically veer 10–50 degrees compared to the prevailing wind direction aloft. The wind direction shear is caused by surface friction that slows the near-surface flow, leading to an imbalance between the large-scale pressure gradient and the Coriolis force, which is lower for slower winds (the Coriolis force is proportional to the velocity components). The wind direction shear is especially relevant when surface friction is large such as over vegetation canopies, urban areas, and rough complex terrain. Buoyancy effects also play an important role in determining the magnitude of the veering angles. Veering angles were found to be larger for the stratified flow typical of nighttime and winter conditions (in the northern hemisphere) and lower for well-mixed convective conditions [25]. Hence, wind direction shear is not uncommon and transport winds may be insufficient to capture smoke dispersion patterns to determine if a prescribed burn has the potential to place smoke on sensitive targets (e.g., hospitals) or reduce road visibility.

2.2.2. More Modern Weather Products

The National Weather Service (NWS) provides hourly weather forecasts 48 h in advance and day/night averages out to 10 days. Hence, information on the expected weather can be used to decide which plot to burn and with what ignition strategy days in advance. The NWS weather forecasts have a horizontal resolution of ∼3 km and capture 4157 public forecast zones (Figure 6).

Currently, fire practitioners use the forecast for the location closest to the site of interest to determine the expected conditions. However, better predictions can be achieved by using the gridded output from weather models instead of point forecasts to gain an understanding of the variability in the winds and other weather variables over the landscape of interest and in relation to populated areas and sensitive locations. For instance, Figure 7 shows the wind profiles from the High Resolution Rapid Refresh (HRRR) reanalysis at 3 km horizontal

resolution. The maximum wind direction difference at 10 m AGL is ∼40 degrees while the maximum wind direction difference across all heights is 65 degrees. Also, several wind profiles show the wind direction shear with height within a couple of hundred meters from the surface. Smoke released in these conditions will travel a more complicated path than is describable with just the surface and transport winds.

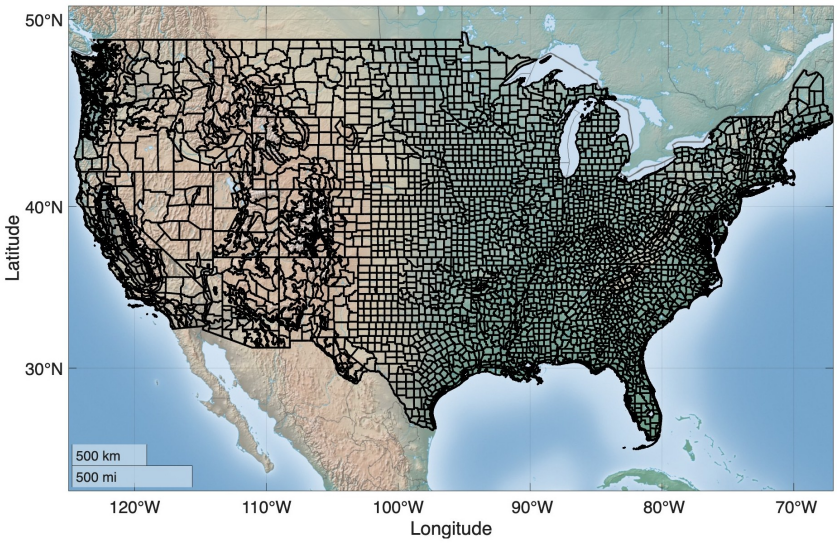

Figure 6. Public forecast zones. Data from [26].

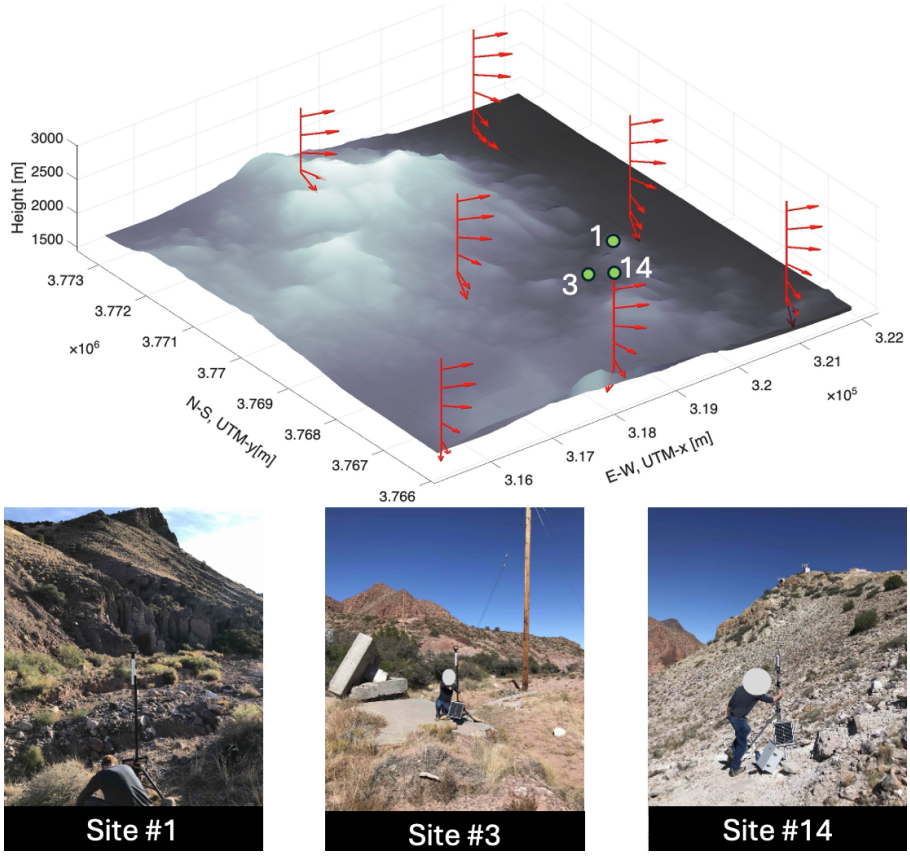

Figure 7. Vertical wind profiles from High Resolution Rapid Refresh (HRRR) at the Energetic Materials Research and Testing Center (EMRTC) site for 1 November 2019, at midnight local time. Several profiles shows wind direction shear with height, with the local topography strongly channeling winds at the surface (see insets to appreciate the steepness of the topography). The mean difference between the surface wind direction and the upper air wind direction is about 100 degrees.

In the U.S. one of the derived weather products is the fire weather forecast, which is used to determine if conditions are favorable for fire growth and smoke dispersion. Fire weather forecasts report information for a geographic area called the fire weather zone (Figure 8) which includes areas within a U.S. state which share relatively uniform climatic and vegetative characteristics that influence fire behavior [27]. These zones differ from public weather zones. The fire weather forecast spans one week, although less information is reported from day 3 forward, and reports the daytime and nighttime winds for the first 24 h and their expected shifts. In reality, winds will not be constant over the fire weather zone, which can be quite large. See Figure A2 for an example of a fire weather forecast.

2.3. Spot Forecasts: Day of the Burn Go/No-Go Decision

Spot forecasts are special forecasts issued for a specific location to help the fire manager decide if the weather conditions are favorable to conduct the burn. They are issued hours before ignition and may be obtained by Fire Control Agencies upon request to the Weather Forecast Offices (WFO) of the NWS. Between 2009 and 2013, about 1800 spot forecasts per month were issued nationwide for either wildfires or prescribed burns, for a total of 103,370 forecasts [28]. Since spot forecasts are issued close to the time of ignition it is impractical to use them to run models in the field.

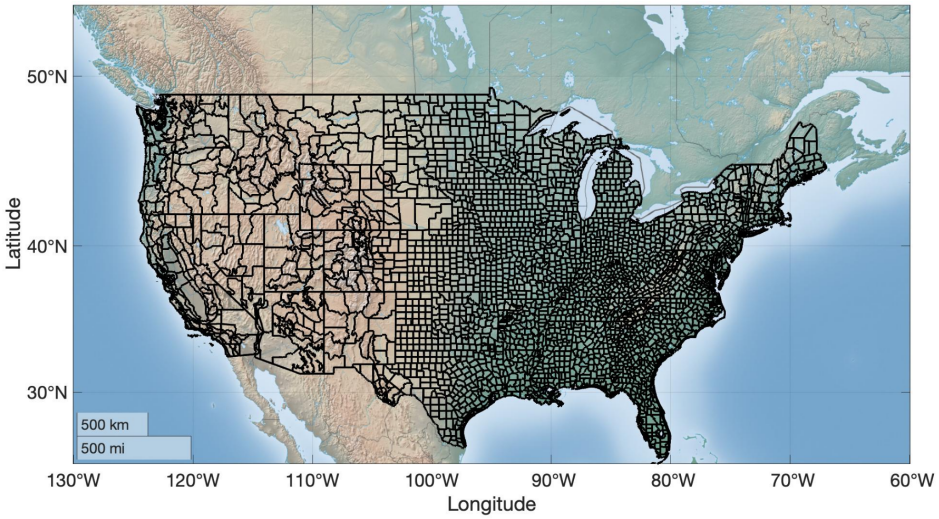

Figure 8. Fire weather zones. Note that the fire zones do not correspond to the public forecast zones in Figure 6. Maximum area = 1.1×10^5 km^2; median area 1.5×10^3 km^2. Data from [29].

While observations are not required, on-site observations regarding dry bulb temperature, relative humidity, and surface winds can assist the WFO [30]. There are two types of weather stations that can be used by the spot forecaster to correct larger scale forecasts with current weather data: the NWS/Federal Aviation Administration (FAA) network and the Remote Automatic Weather Stations (RAWS); see Figure 9. NWS/FAA stations tend to be located at or near airports and the recommended routine reporting time is immediately prior to the top of each hour. The wind speed is reported at 10 m AGL and represents a 2 min average. RAWS are an inter-agency network of surface stations that are primarily used to assess fire danger in remote locations throughout the U.S. Winds are measured at 6.1 m (20 ft) AGL. Winds are collected from 10 min averages prior to the hourly transmission time [31]. At the time of writing, there are 2525 RAWS stations active.

The median distance of the NWS/FAA stations from the RAWS stations is 30 km. Given the high cost of maintaining the networks, Horel and Dong [32] explored if it would be reasonable to eliminate some stations in either the RAWS and NWS/FAA network without degradation in two-dimensional variational data assimilation analyses for temperature,

relative humidity, and wind speed. It was found that the analyses deteriorated less when the removed station was in proximity of other stations. Degradation, expressed as an increase in the error when removing a station to conduct the analysis, was higher than 40% when removing either all RAWS or NWS/FAA stations, implying that the average error was almost doubling. Both networks are therefore needed to provide data for both weather forecasting and decision making related to prescribed fires.

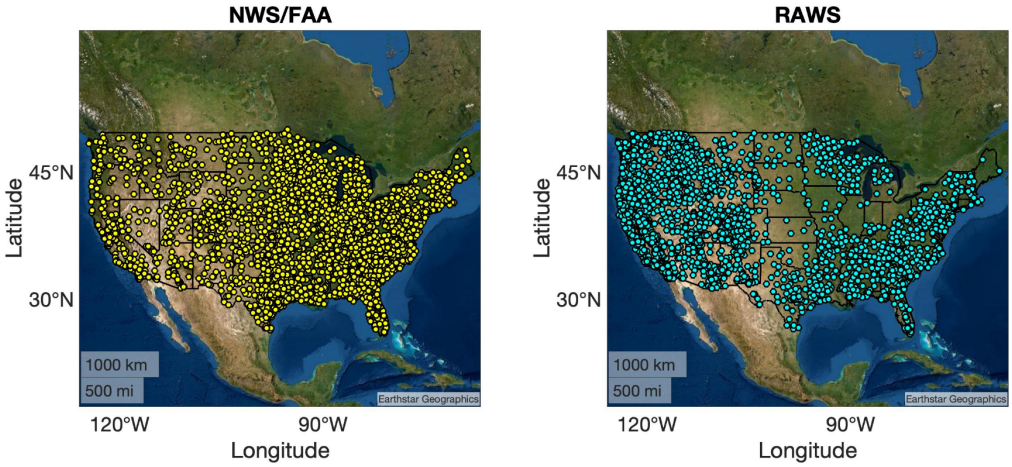

Figure 9. NWS/FAA and RAWS stations for the continental U.S. Data from: Synoptic data [33].

3. Gaps in Existing Climate and Weather Products

This section discusses the gaps in the current forecasting capabilities specific to predicting fire and smoke behavior. The gaps discussed here are the same for both weather and climate forecasts. However, they manifest differently between the two types of forecasts. The main themes discussed here are as follows:

- Downscaling:
  - Spatial downscaling, to enhance the forecast resolution, is particularly desirable in complex terrain to understand local wind patterns and effects that may change fire spread and smoke dispersion.
  - Temporal downscaling is used to enhance time resolution for resolving wind speed and direction shifts in order to capture phenomena like the sea breeze and thermodynamically induced winds on mountain slopes. These phenomena are tied to the diurnal cycle and can lead to wind reversals, transforming a fire flank into a head or pushing the fire back against consumed fuel, leading to drastic changes in fire behavior.
- Bias correction can be used to adjust the forecasted variable to better match measurements.
- Uncertainty quantification is valuable in order to understand the range of variation in the winds due to, but not limited to, errors in initial and boundary conditions, model parameterizations, and data assimilation.

For climate forecasts and seasonal outlooks, local disturbances that will affect future fire and smoke behavior may not be captured because of climate model resolutions. An example disturbance is the occurrence of a large wildfire which suddenly modifies the forest structure and therefore the winds within it. For short term planning the main issue is model resolution in complex terrain, which encompasses all the aforementioned topics. Since the gaps are similar for both short-term planning and day of the burn decisions, the latter section is omitted.

3.1. Climate Forecasts

For prescribed fire planning activities, the feedback from wildfires to the local weather must be understood to account for changes in the landscape's properties that could make a prescribed fire easier or more difficult to manage. The 2018 Camp Fire in California is an example of a wildfire that changed the local weather [34]. The vegetation cover type shifted from evergreen forest and shrub/scrub cover to grasslands and herbaceous vegetation. Satellite data shows the changes in land surface characteristics, measurable through the Normalized Difference Vegetation Index (NDVI), albedo, and land surface temperature (LST). Over the region burned, the green vegetation cover decreased by 20% while the mean daytime LST increased by 2.5 °C.

Wildfires impact the local weather through changes in the interaction between the land surface and the atmosphere. Whenever fire occurs in a landscape, some of its properties change. The duration and magnitude of the disturbance depend on the fire's intensity, duration, and characteristics. Destructive wildfires can affect an area for years as the ecosystem struggles to recover, thus influencing the local weather [35]. Among the changes induced by a wildfire, we find the following [34,36,37]:

- Decreases in evapotranspiration and increases in albedo, where vegetation is replaced by bare ground.
- Changes in temperature and moisture, which depend on the balance between the aforementioned aspects. Usually, the effect of the loss of evapotranspiration is larger than that of the change in albedo, resulting in increased temperatures.
- Soil moisture depletion, with the post-fire dry soils heating up faster.
- Increases in soil hydrophobicity through the removal of surface debris leading to a reduction in water infiltration, and an increase in runoff and soil erosion.
- Canopy-scale wind changes through canopy loss and reduction in leaf area.
- The replacement of an ecosystem by faster-growing, potentially invasive species.
- A build-up of coarse woody fuels on the forest floor that can sustain high-intensity fires.
- Shifts in fuel moisture content. For wildfires that kill the trees while leaving them standing, the moisture content shifts from live fuel moisture (>100% g of water per g of dry fuel) to dead fuel moisture, which depends on the size of the fuel element, the relative humidity, the air temperature, the time of day and season, fuel shading, and the time since the last precipitation. The accurate estimation of fine fuel moisture is critical for computing the fire rate of spread: a 5% error in fine fuel moisture content can lead to a 30–50% increase in fire spread rate [38]. The relationship between fuel size and relative humidity is oftentimes approximated as in Table 2.

Table 2. Dead fuel moisture time lag rules of thumb representing the time it would take to dead fuel to reach 2/3 of the equilibrium with the local environment.

Time Lag	Dead Fuel Diameter
1 h	<0.25 in (0.6 cm)
10 h	0.25–1 in (0.6–2.5 cm)
100 h	1–3 in (2.5–7.6 cm)
1000 h	3–8 in (7.6–20.3 cm)

Overall, these changes may be beneficial for low-to-medium intensity wildfires if leveraged to enhance the ecosystem's resilience. Wilson et al. [35] demonstrated the use of wildfires scars to increase an ecosystem resilience by carrying out prescribed fires using the scars as black. For high-intensity wildfires, the changes listed above may lead to more extensive changes in the local climatology that need to be considered in the planning of

future prescribed fires. For instance, the burnt area may have to be prioritized to reduce snags (dead standing trees). The changes induced by a wildfire may be missed by the climatological outlook because of model resolution (tens of km) but can be discerned through in situ observation and satellite data, as in the case of the Camp Fire [34]. For climate forecasts, the current challenges are downscaling the climate outlook to the area of interest, considering the disturbance, the quantification of the uncertainty in a new climate forecast that considers the disturbance, and its bias correction as past adjustments do not capture the new forest structure.

3.2. Weather Forecasts

Given the resolution of weather forecasts (3 km in the U.S.), many terrain features that impact both winds and fire behavior become underresolved (Figure 10). Wind blockage, recirculations/wakes, and thermodynamically induced winds will be only partially captured and may not represent the winds at the site of interest. For instance, Jiménez and Dudhia [39] found systematic wind direction biases between observations and WRF (at 2 km resolution) over complex terrain. Such biases were not present in the flatter areas of the domain considered. The authors also showed that choosing the closest model point to the measurement site for comparison was not always the best choice. Instead, choosing the closest model point with the most similar terrain features reduced the bias. For instance, the 2019 experimental campaign at the Energetic Materials Research and Testing Center (EMRTC) in New Mexico showed the differences between winds measured within the rugged terrain and the closest airport in Socorro [40]: despite being less than 8 km apart, the wind roses are completely uncorrelated (Figure 11). These examples highlight the importance of downscaling and bias correction to infer the winds at the site of the burn.

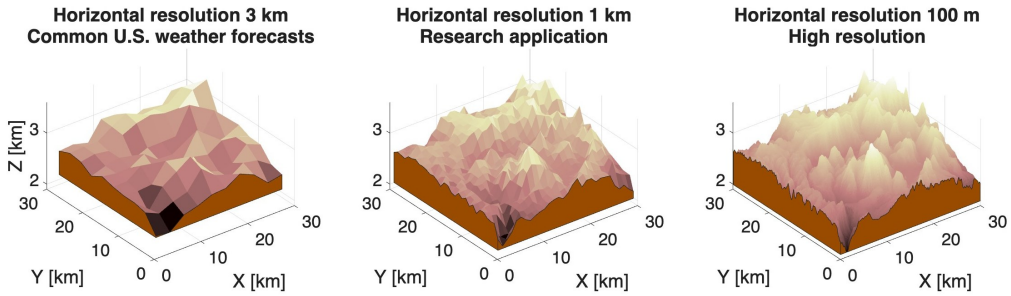

Figure 10. Valles Caldera, NM (35.9 N, 106.5333 W), at different resolutions. Different topographical elements and slopes, which strongly influence fire spread, are captured at the different resolutions.

Another aspect to consider is vertical resolution. Outside of research applications, the first layer of weather forecast models cannot resolve vegetation, which is commonly represented through a season-dependent roughness length, displacement height, and drag. Charney et al. [41] simulated two prescribed fires with and without adjusting the winds for the presence of the canopy while using high vertical resolution (2 m for the lowest 84 m of the atmosphere). The result was that the smoke plume was more vertical when accounting for the presence of the canopy due to the lower in-stand winds and higher air temperatures (by 6–7 K) that were reached within the canopy from the reduced mixing driven by canopy drag. Accordingly, the height reached by the plume was higher for the simulation with the canopy. The plume also tended to persist longer within the canopy. Mallia et al. [17] analyzed WRF simulations without correcting the winds for the presence of the forest canopy and with the canopy parameterization by [42]. When using the canopy parameterization, a lower bias in wind speed was found and the fire spread rate was reduced and closer to the observed rate. In particular, fire spread rate was twice the measured rate when the canopy parameterization was not used. These examples

highlight the importance of correctly estimating the in-stand winds at the burn site through downscaling and bias correction.

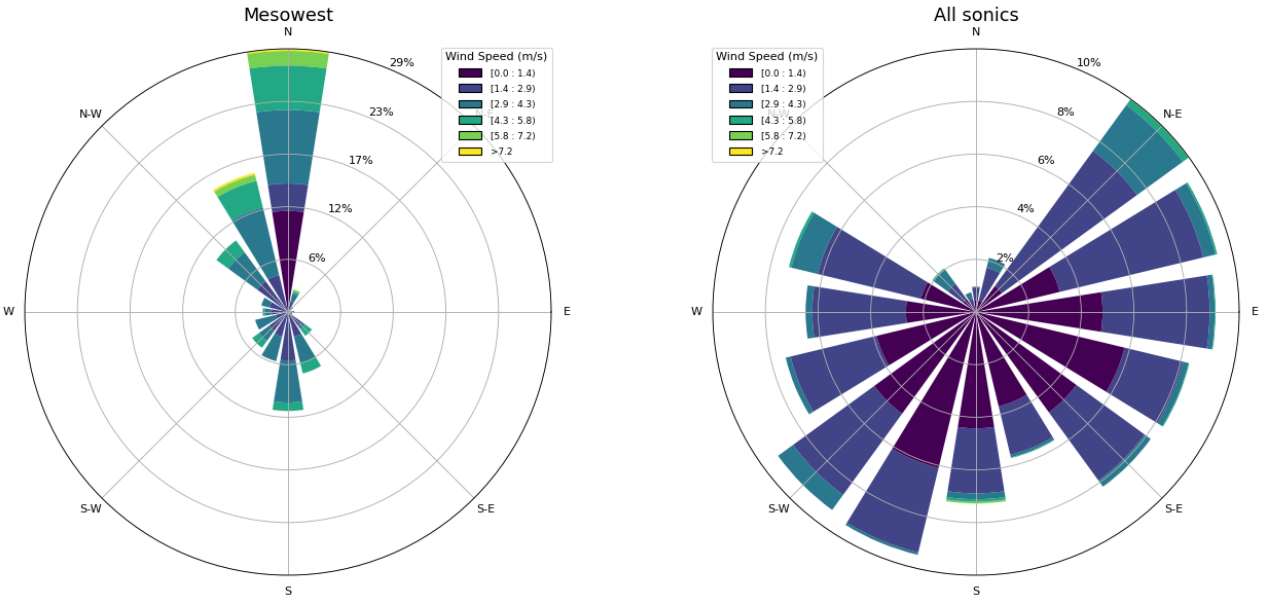

Figure 11. (**Left**): Wind rose for the Socorro Airport KONM station [33]. (**Right**): Wind rose for the wind in the EMRTC mountains (30 min averages) for 1–5 November 2019 [40]. The data from the local terrain is not correlated with the measurements in at the airport.

A weather forecast's accuracy or skill decreases with the lead time, so understanding the range of possible future conditions is paramount. Figure 12 shows an example where the forecasted wind direction changed dramatically during the week leading up to an experimental burn at the Eglin Air Force base. The Monday forecast was used to field some of the instruments, which resulted in sub-optimal locations.

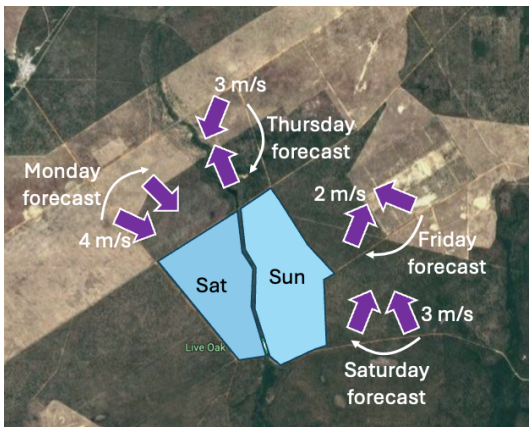

Figure 12. Changes in the weather forecast from [43] for the experimental burn at the Eglin Air Force Base (FL) for the field campaign on 11–12 March 2023. The white arrows indicate the variation in wind direction during the day, considering the hours between 10 a.m. and 4 p.m. local time. The predicted wind direction shifted more than 180 degrees during the week leading up to the experiment. On Saturday, the burn day, the winds were south-westerly.

An ensemble library can be produced around the available forecasts to understand go/no-go conditions and explore alternative ignition strategies. An effort in this direction is BurnPro3D by the University of California San Diego [44]. BurnPro3D lets the user choose a domain of interest, an ignition technique, and the variability in wind speed and direction.

An ensemble is then generated and the data is summarized based on the burn objectives (Figure 13). While today the user has to select the wind uncertainty, in the future this could be derived from past weather statistics and targeted field campaigns.

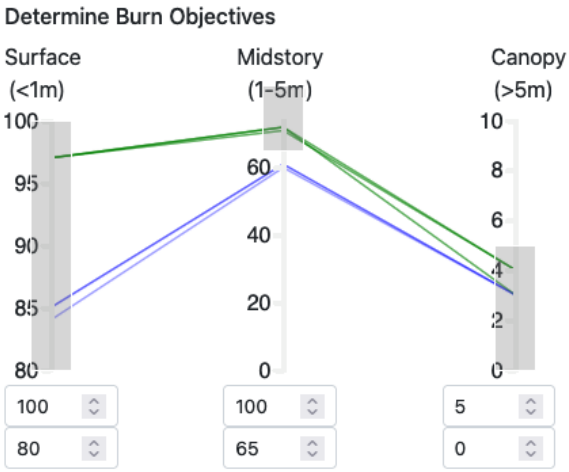

Figure 13. Data analysis of six simulations for the same burn plot and ignition pattern covering two wind speeds and three wind directions. The gray boxes represent the burn objectives for this specific burn unit; green lines represent conditions that lead to burns within prescription while blue lines represent conditions that only partially meet objectives. Red lines (not present) would represent conditions that do not meet the canopy consumption objectives.

4. Emerging Opportunities for Artificial Intelligence and Machine Learning

Artificial intelligence (AI) and machine learning (ML) are uniquely placed to support the needs of next-generation wind modeling for prescribed fire planning and execution because of their ability to quickly analyze large amounts of complex data, describe nonlinear relationships among variables at differing scales and resolutions, and build computationally efficient predictive models. The rapidly growing AI/ML research space has already produced significant results in wind modeling that span wind energy, turbulence, and climate forecasting at a range of scales. However, more work is required to alleviate the needs of fire modeling and planning. For example, much of the recent and relevant ML work has focused on mapping domain information (topography, urban morphology, signed distance fields, and mesh geometry) and other initial conditions (humidity, sparse field measurements, and wind field simulations) to full flow field predictions. Still, the resolution and the features chosen by these studies are insufficient for prescribed fire needs, even for tools from established companies and institutions (see Table 3).

Table 3. Examples of commercial AI solutions. ECMWF-AIFS: European Centre for Medium-Range Weather Forecasts—Artificial Intelligence/Integrated Forecasting System.

Product	Resolution	Reference
ECMWF-AIFS	0.25 deg, 6 h	[45]
Google WeatherNext 2	0.25 deg, hourly	[46]
Tomorrow.io	10, 100, 200 m, Unknown time resolution	[47]
AccuWeather AI	1 km, 1 min	[48]

Since AI/ML is not a standard set of tools and may vary widely in underlying architecture, assumptions, and learning methodology, we summarize four key categories relevant to wind prediction in Appendix C. Irrespective of the specific AI/ML technique adopted, the desired outputs of the chosen AI/ML technique are as follows:

- A 3D wind field at a resolution higher than existing weather or climate forecasts. For complex terrain, this means meter scale in horizontal resolution and winds resolved through the canopy in the vertical direction. Usually, less resolution is necessary above the vegetation, or tens of meters from the ground, as gradients may be less sharp.
- Time series—hourly for climate forecasts and sub-hourly for weather forecasts of wind speed and direction—for capturing phenomena like sea/land breezes and the initiation of thermodynamically induced winds on mountain slopes.

Table 4 presents some common metrics used to validate wind models [49,50]. Since errors between different locations in a domain of interest can compensate or exacerbate each other, it is fundamentally important to assess how these errors ultimately impact fire spread metrics and smoke dispersion. For prescribed fire applications, the rate of spread is not as interesting as a defined front does not usually exist by design. For smoke, since quantitative concentration measurements are usually very sparse, other metrics can be used, for instance comparisons to satellite imagery or video recordings.

Table 4. Metrics commonly used to evaluate a wind model and its impact on fire and smoke outcomes.

Wind Speed	
Mean absolute error (MAE)	Fire spread rate is directly proportional to wind speed, while smoke concentration is inversely proportional.
Root mean square error (RMSE)	Larger errors are penalized more. When compared to MAE, it indicates the presence of outliers.
Mean bias error (MBE)	Assesses a model's tendency to over- or underestimate data, providing a measure of compensating errors.
Factor of X	Ratio between the measured and modeled wind speed, where X is an acceptable factor, e.g., factor of two. Used to assess the fraction of simulated winds with an acceptable error.
Wind direction	
Mean absolute error (MAE)	For uniform winds, it would indicate errors in the smoke trajectory. With heterogeneous winds, errors may compound or cancel each other out.
Fraction $\leq$ X degrees	Fraction of modeled winds within a certain angle of the measurements, usually 10–30 degrees.
Fire	
Ground, midstory, and canopy fuel consumption	Measure of burn effectiveness and negative outcomes (see example in Figure 13)
Smoke	If measurements are available [49]
Same metrics as wind speed	
Correlation coefficient	Strength of the linear association between measurements and model.
Fractional bias (FB)	Measure of the difference between measurements and model.
Smoke	From remote sensing (e.g., satellite)
Smoke cloud top	Measures the height reached by the smoke. Paired with weather forecasts, it determines if the smoke punched through the boundary layer or if it was trapped within. It is an important parameter as it determines smoke ground concentration.
Figure of merit in space	Quantifies the horizontal placement of the simulated vs. modeled plumes. It may not be able to quantify if the plumes are at the same heights.
Smoke peak concentration	Aerosol optical depth can be used to infer the smoke timing and location of the smoke peak concentration from remote sensing to assess if the model is transporting the smoke correctly. As for the figure of merit, the peak could be at different heights between model and reality.

Model validation requires data. Routine measurements from NWS/FAA and RAWS stations can be used together with measurements from different countries (e.g., [50]). A number of field campaigns are also available, e.g., [40,51–54].

The following sections describe how AI/ML can be used to obtain the desired outputs by addressing the gaps identified in Section 3, i.e., downscaling, bias correction, and uncertainty quantification. While these topics are described in separate sections, they are not independent from each other and may be addressed together in practice. In addition, by joining meteorology with AI/ML, the data assimilation limitations of current weather models can be surpassed and a new unprecedented amount of heterogeneous data streams can support higher resolution, more timely, and more reliable forecasts. Fire science still faces unique challenges that existing AI/ML tools have not addressed, which leaves room to develop practical solutions tailored for fire professionals that will have real world impact.

4.1. Downscaling

Numerical Weather Prediction (NWP) and climate model outputs are too coarse for the needs of next-generation prescribed fire models, especially as fire is expanded into new areas with mountainous terrain. The importance of downscaling and real-world consequences can be appreciated by looking at the 2022 Hermits Peak/Calf Canyon wildfire, the largest in New Mexico history, which started as a prescribed burn. The post-incident analysis reads, "Collective experience from in-person discussions with personnel in the prescribed fire organization suggest that forecast predictions from the National Weather Service are seldom representative of what is observed at the site because of the terrain influences overriding the numerical weather predictions" [55]. This account highlights the need for forecasts to be downscaled to produce wind information at higher spatial and/or temporal resolution. Downscaling in this context often falls into the following categories [56]:

- Dynamical downscaling, in which a higher-resolution NWP model is run over the area of interest. This is often prohibitive because of the computational resources required and operational constraints. Since a higher resolution requires smaller time steps, the forecast may become available after it is of interest at the resolutions required by prescribed fire applications.
- Statistical downscaling, which involves deriving transfer functions that relate lower resolution weather forecast to higher resolution measurements, usually surface winds.
- Combined statistical/dynamical downscaling that leverages both techniques.
- The analog method, in which the present is compared to the past and the closest analog is used [57].

4.1.1. Spatial Downscaling

Existing AI/ML techniques are insufficient for fire modeling because they were developed for different applications, like wind energy or urban flow modeling, and therefore the following is true:

- Only one variable is downscaled, e.g., wind speed or temperature [58].
- The variable of interest is downscaled only at one point, e.g., the height of the wind turbines or the location of the local weather station, or at one reference height, e.g., 2 m AGL temperature [59].
- Only the distribution of a variable over a year is downscaled to predict for instance power output from a wind farm [60].
- The downscaling method only ingests the variables forecasted by the NWP model (temperatures and winds) and no other local information is included [61]. This is particularly relevant for mountainous terrain where topography plays a big role in generating local phenomena. For topography, derived quantities like the slope, aspect,

and distance from the coastline, and not just the elevation, may have to be included for a successful downscaling.
- The target resolution is still too coarse for prescribed fire applications, e.g., [50,62,63].
- The AI/ML technique was developed for urban environments instead of complex terrain, e.g., [64].
- While promising, the developed technique has not been applied to regions outside the training region to demonstrate generalization [50,65].

A direct approach is to train the AI/ML with dense local measurements without including any information on the fuel or the topography. Being purely data-driven, the method is only applicable to the area of interest, but it may work well there, e.g., [50]. The limitation is the amount of data required, especially as prescribed fire is applied to new, previously unburnt areas where wind measurements are sparse.

An increasingly successful approach includes terrain effects, representations, meshes, or other geological and geometric descriptors as input. A number of ML-driven research efforts in wind flow field prediction have explored this to varying degrees of success, some notably in urban flow modeling [66–68]. Common inputs have included the digital elevation model (DEM), signed distance fields (SDFs) which describe the distance at any point in a domain to the nearest surface, geological descriptors such as surface roughness, and geometrical or computational meshes/point clouds. However, other representations may be relevant as input fields for ML such as a geomorphon labeling, which identifies tiles in a DEM as a set of basic shapes. These geomorphons are defined as terrain building blocks that, when combined in various configurations, can represent nearly any complex terrain feature encountered in the real world and may describe the majority of the flow. Examples of basis shapes for parameterizing winds in mountainous terrain are [69] ridges (linear maxima) and valleys (linear minima), pits (local minima) and peaks (local maxima), and constant slopes; see Figure 14. Another representation may be found via reducing the terrain via a basis expansion, such as through principal component analysis (PCA), which may aid in identifying low- or high-frequency content for reproducing wind fields. In this case, a number of techniques can be used to identify the relationships between winds and topography to model the flow over each basis shape from high-fidelity model simulations. The solution on the real complex terrain of the site of interest becomes a combination of the physics of individual, easier to compute, discrete shapes. This method can achieve generalization because it involves learning the flow dynamics over basis shapes and not entire topographies (which are location specific). This approach is more complex and may not work as well as models trained on local measurements specific to an area but has the potential to be generalizable.

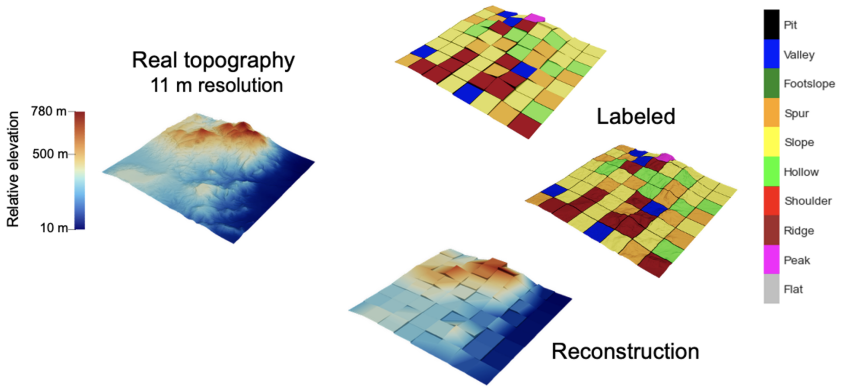

Figure 14. (**Left**): Topography of the mountain range near Socorro, New Mexico, for a domain size of 6.6 × 6.6 km at 11 m horizontal resolution (z-direction not to scale to emphasize terrain features). (**Right**): Geomorphon labeled terrain and reconstructed geomorphon terrain.

4.1.2. Temporal Downscaling

Burn plot prioritization at the regional scale currently uses climate outlooks to identify the months/seasons in which relevant weather variables will likely be within the prescription window. This analysis does not consider diurnal variations and, therefore, the possible development of undesirable conditions throughout the day. Since not all burns are concluded over a short period of time ($\leq$1 h), understanding the possible evolution of the winds during the burn itself is important.

One solution is deriving synthetic time series of wind speed and direction that can be fed directly into fire models. Current methods like [70] start from measured time series at a given location, and data is aggregated by month and hour to derive the distribution of wind speed and direction. Ideally, the different mechanisms that generate winds are separated and predicted independently, e.g., downslope drainage flow and land/sea breeze [71]. For instance, in [71], ten distinct disjoint components were identified for an Italian airport on the sea, seven of which varied strongly with the time of day while three did not. AI/ML algorithms are well-positioned to support this classification step to recognize the different mechanisms resulting in a certain wind speed and direction and their diurnal pattern.

Current methods are based on local meteorological observations, but in the case of prescribed fires, data may not be available for remote sites of interest. One could generalize the approach using reanalysis data, e.g., from the ECMWF Reanalysis version 5 (ERA5), which provides global hourly estimates of a large number of atmospheric, land, and oceanic climate variables at a 9 km resolution. Reanalysis using higher-resolution models can also be achieved, e.g., with the Wind Integration National Dataset Toolkit [72], which has 2–4-km spatial resolution and 5 min to hourly temporal resolution (continental U.S.).

Regardless of the method and data chosen to generate the synthetic time series, the uncertainty in computed winds must be reported and accounted for in fire modeling. Since lightweight models that can capture both the physics of prescribed fires and run in an ensemble fashion were developed only over the last five years (e.g., [7]), there is a lack of comprehensive studies on how to use synthetic time series and their uncertainty.

4.2. Bias Correction

Bias correction is the process of correcting the forecasted variable(s) to better match the measurement(s), thus improving the forecast accuracy. Biases can be introduced in the forecast because of the challenges related to the location (e.g., complex terrain and land/water interface), the forecast lead time, initial conditions errors, boundary conditions errors, and model errors due to the numerics and the representation of physical phenomena [73].

Several statistical correction methods have been devised for bias correction, which in general are based on correlating the historical prediction error to one or more input variables, which can be state-dependent predictors, i.e., outputs of the forecast, or static predictors, i.e., variables independent from the forecast like topography and time indicators (day of the year) [59].

Bias correction can be applied to the whole forecast or only at locations of interest. Point correction methods are focused on correcting the forecast at individual weather observation stations and not correcting the whole forecast over a region. Hence, these methods are not well suited to use high-dimensional structured spatial data from an NWP model. In addition, these methods require measurements at the location of interest and, therefore, suffer from difficult generalization. Whole-forecast bias correction involves correcting for the difference between the NWP prediction and a reanalysis prediction, usually using ERA5 dataset as the ground truth [74]. Different ML approaches can be leveraged to correct the bias in regional wind fields. For instance, Pang et al. [75] carried out bias correction through a diffusion model/U-Net hybrid network while Zhang et al. [76]

generated real-time correction of the horizontal wind components via a spatiotemporal deep learning model. While these methods are still tied to the training site, they offer insight into how to move forward for a more general inference. Scher and Messori [77] highlight some important aspects related to ML training with reanalysis data. First, the dataset used for the ML training needs to be homogeneous, i.e., it needs to be computed with one version of the weather prediction model of choice instead of multiple versions over the years. Existing reanalysis products may or may not satisfy this requirement. Second, one has to choose the input variables for the ML model and only certain pressure levels may be used instead of the full three-dimensional grid of the NWP model to reduce computational requirements. Third, the ML model may be trained with data related to a specific area of the globe because of the trade-off between data size and completeness. The area chosen must be representative of the domain of interest. The training dataset can also be divided into "weather types" to improve bias correction [78]. Similar considerations in the ML context are thoroughly addressed in the recent work of [79].

As with downscaling, the choice of the input parameters strongly affects the accuracy of any technique. A variable that explains most of the bias in one region may be uninfluential in a different one because of local features. Building a generalized AI/ML technique that works across different regions and different weather patterns may therefore be more involved and more data intensive than correcting for a specific area of interest.

4.3. Uncertainty Quantification

Uncertainty in weather represents a measure of the confidence of a certain outcome and is determined by the spread of a certain variable across ensemble simulations. Weather forecasts are always computed from ensembles but the individual model runs and the spread across runs of variables, like wind speed and temperature, are usually not presented for general consumption. The uncertainty for selected variables can be found for instance in form of maps at [80], selecting "GEFS-MEAN-SPRD" as the model type (Global Ensemble Forecast System Mean and Spread). The wind direction uncertainty is not presented and must be retrieved from the ensemble members raw data.

The knowledge of the uncertainty in the mean wind speed and direction can be incorporated into prescribed fire modeling by running ensemble simulations that translate the uncertainty into prescription effectiveness, probability of escape, and probability of exceeding smoke concentration/dosage thresholds.

In practice, this is an exercise in error propagation for which established techniques already exist. In general, the uncertainty for each variable is fitted with a distribution function from which each variable is sampled. The sampling can cover the entire range of the selected variable uniformly or random sampling techniques can be used (e.g., Monte Carlo and Latin hypercube). The fire behavior and smoke transport models are then run using each combination of the uncertain input variables. Metrics are established to compare the different realizations (e.g., Table 4). The procedure can be repeated to understand the effect of different ignition strategies to then select the most robust. Alternatively, a subset of "good" weather/ignition strategy pairs are selected and compared to the day of the burn conditions.

Work has been undertaken to connect the uncertainty in winds to the overlap of the simulated wildfire's patterns. This is, however, not relevant for prescribed fires, where the fire spreads within a predefined burn unit and escapes are easy to detect. As observed for temporal downscaling, we are now at the time where computational power and model capabilities allow for the first time to run ensemble wildland fire/smoke simulations. Hence, studies specific to prescribed fires do not exist. There are two main ways in which AI/ML can help. One way is to create a tool specific for a geographic area. In this case,

a fire/smoke model can be run for a set of representative wind speeds and directions on the characteristic fuels and slopes of the area and the AI/ML tool could interpolate across existing runs. The training would have to be repeated any time any of the input conditions deviate "significantly" from those of the training dataset, but the tool will likely work very well for the area of interest. The second approach is to build a more general tool. This may require continuous learning as fire is moved into new ecosystems or topographies and new conditions are encountered. The advantage is that this could be framed as a community effort where no one institution takes on the burden to run "all" the possible combinations of input parameters, but rather, the training data is shared and the AI/ML model expanded in time as new data becomes available. In the U.S., the Department of Defense has supported the creation of a website where data from experimental prescribed burns is shared [81]. A similar place could be a created to host the training datasets and the derived AI/ML model(s).

5. Conclusions and Future Directions

Prescribed fire operations are high-impact activities and an increased acreage burnt can only be achieved by expanding existing burn windows. The modeling of fire spread and smoke dispersion can support the identification of go/no-go conditions, planning for optimal ignition strategy, and burn plot prioritization at the landscape scales. These activities occur over different temporal scales, from day of the burn, to a week in advance, to months/years in advance.

One factor limiting the expansion of burn windows concerns the accuracy, resolution, and reliability of wind forecasts that feed fire behavior and smoke dispersion models. Current wind products, like surface and transport winds, are too limited to serve next-generation fire models. The 3D nature of operational forecasts makes them more appealing to capture local changes in wind speed and direction, but they are still too coarse, both spatially (about 3 km in the U.S.) and temporally (hourly) to resolve the micro-scale flow structures that govern fire spread in complex terrain. This leads to over-conservatism, which reduces the number of burn days and increases planning uncertainty.

This paper identified three priority research gaps in weather and climate forecasting specific to prescribed fire operations: spatial and temporal downscaling, bias correction, and uncertainty quantification. AI/ML offers tools to close these gaps with recent advances showing significant potential. By providing high-resolution, bias-corrected, probabilistic wind fields AI/ML-enhanced forecasts can feed next-generation prescribed fire models to generate ensembles within tools such as BurnPro3D. This coupling enables deriving expanded, science-based burn windows and deriving a set of optimal ignition patterns that account for expected wind variability.

While AI/ML predictive capabilities for atmospheric flow modeling are still evolving, both the power of computational hardware and AI/ML modeling approaches have advanced rapidly in recent years, such that what was not possible just a decade ago is now attainable. Historically, computational power has been limited for these efforts, constraining both the generation of high-resolution numerical simulations and the training efficiency of high-parameter ML architectures. For instance, NVIDIA GPU's went from 3.5 TFLOP/s with the 2014 NVIDIA GTX 970 to 60 TFLOP/s with the 2022 NVIDIA H100, an almost 20× increase in raw computational power. Google TPU jumped from 45 TFLOP/s with the v2 version in 2019 to 2.5 PFLOP/s with the v4 version in 2023, a 55× increase. These performance gains also enable more expressive ML architectures. In particular, researchers have only recently begun to explore modern, state-of-the-art architectures such as vision transformer models [65] and graph networks [68,82] on detailed CFD simulations for wind forecasting problems. These advancements indicate that we may now adopt increasingly

more expressive architectures trained on higher-resolution simulations for the prediction for wind flow over complex terrain.

In summary, the convergence of high-resolution meteorological modeling, emerging AI/ML methodologies, and next-generation fire behavior models creates a pathway to reduce conservatism in prescribed fire planning while maintaining safety. The creation of effective solutions will require the development of robust and reproducible training datasets and sustained collaboration among atmospheric scientists, fire ecologists, data science engineers, and land management agencies. The envisioned AI/ML-driven wind-forecasting framework can then supply needed data to existing and future prescribed fire models.

Author Contributions: Conceptualization, S.B.; writing—original draft preparation, S.B., J.E.S. and S.X.C.; data curation, S.B., J.E.S., D.R. and D.J.R.; project administration, S.B.; and funding acquisition, S.B. and A.T.M. All authors have read and agreed to the published version of the manuscript.

Funding: The research presented in this article related to current and next-generation weather products was supported by the Department of Defense Environmental Security Technology Certification Program (ESTCP) under project number RC23-B6-7656. The research presented in this article related to Artificial Intelligence and Machine Learning opportunities was supported by the Laboratory Directed Research and Development program of Los Alamos National Laboratory (LANL) under project number 20250137ER.

Data Availability Statement: No new data were created or analyzed in this study.

Conflicts of Interest: The authors declare no conflicts of interest. The funders had no role in the design of the study; in the collection, analyses, or interpretation of data; in the writing of the manuscript; or in the decision to publish the results.

Abbreviations

The following abbreviations are used in this manuscript:

AGL	Above Ground Level
AI	Artificial Intelligence
AIFS	Artificial Intelligence/Integrated Forecasting System
ECMWF	European Centre for Medium-Range Weather Forecasts
ERA5	ECMWF Reanalysis v5
ESTCP	Environmental Security Technology Certification Program
FAA	Federal Aviation Administration
FNO	Fourier neural operator
GEFS-MEAN-SPRD	Global Ensemble Forecast System Mean and Spread
HRRR	High Resolution Rapid Refresh
LES	Large Eddy Simulation
ML	Machine Learning
NWP	Numerical Weather Predictions
NWS	National Weather Service
PCA	Principal component analysis
PDE	Partial differential equation
PIML	Physics Informed Machine Learning
RAWS	Remote Automatic Weather Stations
U-Net	Convolutional neural network that was developed for image segmentation
WFO	Weather Forecast Offices
WRF	Weather Research and Forecasting
WRF-SFIRE	Coupled atmosphere-wildfire model, which combines WRF with a fire-spread model

Appendix A. Burn Window

Description of Environmental Parameters Needed to Produce Desired Fire Behavior (Listed parameters are for example only. Chose those that are pertinent to your situation)	Fuels Within the Project or Burn Unit Boundary			
	Dormant Season		Growing Season	
	Low Fire Intensity	High Fire Intensity	Low Fire Intensity	High Fire Intensity
TEMPERATURE (‘F)	40	75	70	95
RELATIVE HUMIDITY (%)	60	18	70	16
20 FT. WINDSPEED	4	20	4	20
WIND DIRECTION	Variable – See Matrix			
CLOUD COVER	50%	0%	55%	0%
KBDI (SOIL MOISTURE)	100	550	100	550
DAYS SINCE RAIN	Variable – See Matrix			
1 HOUR FUEL MOISTURE	18	5	20	6
DISPERSION INDEX	25+			
MIXING HEIGHT	Minimum: 1700’			
TRANSPORT WINDSPEED	6 – 25 MPH			

Figure A1. Example of a burn window for a site in the south-east U.S.

Appendix B. Fire Weather Forecasts

Fire Weather Information for zone NMZ120

Station	Sky	Temp	DP	RH	Wind
KABQ	Clear	13	10	82	calm
KSAF	Clear	11	8	82	N15
KLAM	Clear	10.4	7.1	80	calm
KAEG	Clear	11	10	94	calm

DISCUSSION...

There are no critical fire weather conditions expected for at least the next seven days. Showers and storms will form again today over northeast NM and the southern high terrain. There is a moderate risk for burn scar flash flooding in the Ruidoso area today. A series of backdoor cold fronts entering eastern NM will keep temperatures cool through Wednesday with gusty winds at times. Thursday will be dry and warm for central and eastern NM while storm chances increase over western NM. An unsettled weather pattern may return Friday through early next week with more showers and storms possible.

.....
Experimental Max RFTI, Ventilation category, mixing height and transport winds for each Fire Weather Zone are based on the following points. Note: Maximum transport winds may not occur at the same time as maximum mixing heights.

Zone 101...Farmington.....5500 ft MSL
Zone 120...Jemez RAWS.....8000 ft MSL
Zone 121...Wild River RAWS..7500 ft MSL
Zone 122...Cimarron RAWS....8900 ft MSL
Zone 123...Las Vegas.....6850 ft MSL
Zone 104...Clayton.....5000 ft MSL
Zone 105...Grants.....6600 ft MSL
Zone 106...Albuquerque.....5300 ft MSL
Zone 124...Mountainair.....6600 ft MSL
Zone 125...Santa Rosa.....4700 ft MSL
Zone 126...Tucumcari.....4050 ft MSL
Zone 109...Magdalena RAWS...8450 ft MSL

Ventilation categories are determined by criteria established by each state.

NMZ120-232100-
North Central Mountains-
210 AM MDT Tue Sep 23 2025

.TODAY...
* Sky/Weather.....Mostly sunny. Chance of showers and thunderstorms in the afternoon.
* Max Temperature.....
* Above 8000 ft....59-64.
* Below 8000 ft....69-74.
* 24 hr Trend.....Up 4 degrees.
* Min Humidity.....
* Above 8000 ft....25-35 pct.
* Below 8000 ft....20-25 pct.
* 24 hr Trend.....Down 19 pct.
* Wind...20 Foot.....West 10 to 15 mph. Gusts up to 30 mph.
* 10000 ft MSL Wind...West 10 to 20 mph.
* Chance of Precip....40 pct.
* Mixing Height.....9000 ft agl.
* Transport Winds.....West 20 knots.
* Ventilation Cat.....Excellent/173600 knot-ft.
* Exp. Max RFTI.....0.

.TONIGHT...
* Sky/Weather.....Mostly clear.
* Min Temperature.....
* Above 8000 ft....33-38.
* Below 8000 ft....37-42.
* 24 hr Trend.....Down 4 degrees.
* Max Humidity.....
* Above 8000 ft....66-86 pct.
* Below 8000 ft....68-88 pct.
* 24 hr Trend.....Down 17 pct.
* Wind...20 Foot.....Northwest 10 to 15 mph shifting to the east after midnight.
* 10000 ft MSL Wind...West 5 to 15 mph shifting to the south after midnight.
* Chance of Precip....0 pct.

.WEDNESDAY...
* Sky/Weather.....Mostly sunny.
* Max Temperature.....
* Above 8000 ft....58-63.
* Below 8000 ft....68-73.
* 24 hr Trend.....Little change.
* Min Humidity.....
* Above 8000 ft....28-38 pct.
* Below 8000 ft....23-33 pct.
* 24 hr Trend.....Up 4 pct.
* Wind...20 Foot.....East around 10 mph shifting to the south in the afternoon.
* 10000 ft MSL Wind...South 5 to 15 mph.
* Chance of Precip....0 pct.
* Mixing Height.....6500 ft agl.
* Transport Winds.....West 5 knots.
* Ventilation Cat.....Poor/34200 knot-ft.
* Exp. Max RFTI.....0.

.FORECAST DAYS 3 THROUGH 5...
.THURSDAY...Mostly sunny. Highs 72 to 77. Southwest winds around 10 mph. Minimum Humidity 18 to 28 percent.
.FRIDAY...Partly cloudy. Chance of rain showers. Highs 72 to 77. West winds around 10 mph. Minimum Humidity 20 to 30 percent.
.SATURDAY...Partly cloudy. Chance of rain showers and slight chance of thunderstorms. Highs 71 to 76. Southeast winds around 10 mph. Minimum Humidity 23 to 33 percent.

Figure A2. Fire weather forecast for NMZ120 (northern New Mexico) for 23 September 2025 [83].

Appendix C. AI/ML Techniques

Four key categories relevant to discovery in the field of wind-prediction are as follows:

1. Operator-based methods bypass slow, traditional numerical solvers for partial differential equations (PDEs) by learning the PDE's solutions. They use architectures such as the Fourier neural operator (FNO) [84]. These methods have more recently demonstrated wide-spread success across fields of computational fluid dynamics, climate science, and computer vision for turbulence and wind flow problems.
2. Generative learning strategies attempt to create new, realistic-looking wind fields and other coupled flow data from existing simulations and datasets by employing architectures such as generative adversarial networks or diffusion models [85]. These can also be used to predict statistical uncertainty information via ensembles of this new data, useful in cases where local variability in a weather forecast is not well-known.
3. Physics-informed machine learning (PIML) methods use physics information in a wide range of architectures, often utilizing the strong spatio-temporal patterns inherent in terrain and flow data, and using hybrids of convolutional neural networks, U-Nets, and vision transformers in conjunction with the knowledge of the physics to generate constrained outputs. For instance, Kashinath et al. [86] list ten ways to incorporate physics into AI/ML. Some notable methods are (1) the use of physics-based regularizations, in which the AI/ML includes user-specified regularizations to avoid overfitting by introducing physics-based terms in the loss function, (2) custom-designed neural network architectures that include a layer enforcing conservation laws, and (3) physics-based modeling frameworks where the AI/ML is used to represent terms that are subgrid or not well understood.
4. Graph/mesh-based learning utilize graph representations of meshes, topography labels, buildings, sensors, etc., to enable the coupling of these graphs to other inputs and use tailored neural networks to learn the mapping to flow predictions [87]. Graphs can also enable linkages between static inputs, like wind stations, and dynamic inputs, such as wind velocity fields.

References

1. Rothermel, R.C. *A Mathematical Model for Predicting Fire Spread in Wildland Fuels*; Intermountain Forest & Range Experiment Station, Forest Service, US: Ogden, UT, USA, 1972; Volume 115.
2. Puig-Gironès, R.; Palmero-Iniesta, M.; Fernandes, P.M.; Oliveras Menor, I.; Ascoli, D.; Kelly, L.T.; Charles-Dominique, T.; Regos, A.; Harrison, S.; Armenteras, D.; et al. The use of fire to preserve biodiversity under novel fire regimes. *Philos. Trans. B* **2025**, *380*, 20230449. [CrossRef] [PubMed]
3. NWC Group. Stand Replacing Fire | NWCG—nwcg.gov. Available online: https://www.nwcg.gov/publications/pms205/nwcg-glossary-of-wildland-fire-pms-205/stand-replacing-fire-19 (accessed on 18 January 2026).
4. Hiers, J.K.; O'Brien, J.J.; Varner, J.M.; Butler, B.W.; Dickinson, M.; Furman, J.; Gallagher, M.; Godwin, D.; Goodrick, S.L.; Hood, S.M.; et al. Prescribed fire science: The case for a refined research agenda. *Fire Ecol.* **2020**, *16*, 11. [CrossRef]
5. Zeng, P.; Takahashi, H. A first-order closure model for the wind flow within and above vegetation canopies. *Agric. For. Meteorol.* **2000**, *103*, 301–313. [CrossRef]
6. Linn, R.R.; Cunningham, P. Numerical simulations of grass fires using a coupled atmosphere–fire model: Basic fire behavior and dependence on wind speed. *J. Geophys. Res. Atmos.* **2005**, *110*, D13107. [CrossRef]
7. Linn, R.R.; Goodrick, S.L.; Brambilla, S.; Brown, M.J.; Middleton, R.S.; O'Brien, J.J.; Hiers, J.K. QUIC-Fire: A fast-running simulation tool for prescribed fire planning. *Environ. Model. Softw.* **2020**, *125*, 104616. [CrossRef]
8. Kupfer, J.A.; Terando, A.J.; Gao, P.; Teske, C.; Hiers, J.K. Climate change projected to reduce prescribed burning opportunities in the south-eastern United States. *Int. J. Wildland Fire* **2020**, *29*, 764–778. [CrossRef]
9. Clarke, H.; Tran, B.; Boer, M.M.; Price, O.; Kenny, B.; Bradstock, R. Climate change effects on the frequency, seasonality and interannual variability of suitable prescribed burning weather conditions in south-eastern Australia. *Agric. For. Meteorol.* **2019**, *271*, 148–157. [CrossRef]

10. Linn, R.R.; Sieg, C.H.; Hoffman, C.M.; Winterkamp, J.L.; McMillin, J.D. Modeling wind fields and fire propagation following bark beetle outbreaks in spatially heterogeneous pinyon-juniper woodland fuel complexes. *Agric. For. Meteorol.* **2013**, *173*, 139–153. [CrossRef]
11. Lavdas, L.G. *Program VSMOKE-Users Manual*; Southern Research Station: Asheville, NC, USA, 1996; Volume 6.
12. Brambilla, S.; Rojas, D.; Robinson, D.J.; Josephson, A.J.; Nelson, M.A.; Linn, R.R. Modeling the impact of smoke from prescribed fire on road visibility. *Environ. Model. Softw.* **2025**, *191*, 106510. [CrossRef]
13. Cionco, R.M. A mathematical model for air flow in a vegetative canopy. *J. Appl. Meteorol. (1962–1982)* **1965**, *4*, 517–522. [CrossRef]
14. Cionco, R.M. Analysis of canopy index values for various canopy densities. *Bound.-Layer Meteorol.* **1978**, *15*, 81–93. [CrossRef]
15. Albini, F.A. *Estimating Windspeeds for Predicting Wildland Fire Behavior*; Intermountain Forest and Range Experiment Station, Forest Service, U.S. Department of Agriculture: Ogden, UT, USA, 1979; Volume 221.
16. Moon, K.; Duff, T.; Tolhurst, K. Sub-canopy forest winds: Understanding wind profiles for fire behaviour simulation. *Fire Saf. J.* **2019**, *105*, 320–329. [CrossRef]
17. Mallia, D.V.; Kochanski, A.K.; Urbanski, S.P.; Mandel, J.; Farguell, A.; Krueger, S.K. Incorporating a canopy parameterization within a coupled fire-atmosphere model to improve a smoke simulation for a prescribed burn. *Atmosphere* **2020**, *11*, 832. [CrossRef]
18. Waldrop, T.A.; Goodrick, S.L. *Introduction to Prescribed Fire in Southern Ecosystems*; Forest Service, Research & Development, Southern Research Station: Asheville, NC, USA, 2018.
19. Hanna, S.R.; Britter, R.E. *Wind Flow and Vapor Cloud Dispersion at Industrial and Urban Sites*; John Wiley & Sons: Hoboken, NJ, USA, 2010.
20. Wikipedia. Marking Your Work with a CC License-Creative Commons—Wiki.creativecommons.org. Available online: https://wiki.creativecommons.org/wiki/Marking_your_work_with_a_CC_license (accessed on 18 January 2026).
21. Hess, G.; Garratt, J. Evaluating models of the neutral, barotropic planetary boundary layer using integral measures: Part I. Overview. *Bound.-Layer Meteorol.* **2002**, *104*, 333–358. [CrossRef]
22. Pimont, F.; Dupuy, J.L.; Linn, R.R.; Sauer, J.A.; Muñoz-Esparza, D. Pressure-gradient forcing methods for large-eddy simulations of flows in the lower atmospheric boundary layer. *Atmosphere* **2020**, *11*, 1343. [CrossRef]
23. Jiang, Q.; Wang, S.; Sullivan, P. Large-eddy simulation study of log laws in a neutral Ekman boundary layer. *J. Atmos. Sci.* **2018**, *75*, 1873–1889. [CrossRef]
24. Constantin, A.; Johnson, R. Atmospheric Ekman flows with variable eddy viscosity. *Bound.-Layer Meteorol.* **2019**, *170*, 395–414. [CrossRef]
25. Peña, A.; Floors, R.; Gryning, S.E. The Høvsøre tall wind-profile experiment: A description of wind profile observations in the atmospheric boundary layer. *Bound.-Layer Meteorol.* **2014**, *150*, 69–89. [CrossRef]
26. National Weather Service. NWS Public Forecast Zones—Weather.gov. Available online: https://www.weather.gov/gis/publiczones (accessed on 18 December 2025).
27. NWC Group. NWCG Guide to Fire Weather Forecasts: Types of Fire Weather Forecasts. Available online: https://www.nwcg.gov/publications/pms425/3-types-of-fire-weather-forecasts (accessed on 18 January 2026).
28. Lammers, M.R. Verification of National Weather Service spot forecasts using surface observations. *J. Oper. Meteorol.* **2014**, *2*, 246–264. [CrossRef]
29. National Weather Service. NWS Fire Weather Zones—Weather.gov. Available online: https://www.weather.gov/gis/FireZones (accessed on 20 September 2025).
30. National Weather Service. Spot Forecast Instructions—Weather.gov. Available online: https://www.weather.gov/sew/SpotForecastInstructions (accessed on 27 October 2025).
31. Brewer, M.J.; Clements, C.B. The 2018 Camp Fire: Meteorological analysis using in situ observations and numerical simulations. *Atmosphere* **2019**, *11*, 47. [CrossRef]
32. Horel, J.D.; Dong, X. An evaluation of the distribution of Remote Automated Weather Stations (RAWS). *J. Appl. Meteorol. Climatol.* **2010**, *49*, 1563–1578. [CrossRef]
33. Synoptics. Home Page—Synopticdata.com. Available online: https://synopticdata.com (accessed on 18 January 2026).
34. Blackford, A.; Cowan, T.; Nair, U. VEDA Dashboard—Earthdata.nasa.gov. Available online: https://www.earthdata.nasa.gov/dashboard/stories/burn-scar (accessed on 18 January 2026).
35. Wilson, K.N.; Shive, K.L.; Williams, J.N.; North, M.P.; Coppoletta, M.; Hendershot, J.N.; Stanley, C.K. Perspectives: The pace and scale challenge: Leveraging wildfire footprints to increase forest resilience to future high-severity fire. *For. Ecol. Manag.* **2026**, *603*, 123443. [CrossRef]
36. Holden, S.R.; Berhe, A.A.; Treseder, K.K. Decreases in soil moisture and organic matter quality suppress microbial decomposition following a boreal forest fire. *Soil Biol. Biochem.* **2015**, *87*, 1–9. [CrossRef]

37. Clark, M.L.; Hakkenberg, C.R.; Bailey, T.; Burns, P.; Goetz, S. Changes in GEDI-based measures of forest structure after large California wildfires relative to pre-fire conditions. *Remote. Sens. Environ.* **2025**, *323*, 114718. [CrossRef]
38. Jolly, W.M.; Brenner, J.D.; Long, A.J. SimpleFFMC: A New Calculator for Fine Fuel Moisture Content | Fire Research and Management Exchange System—Frames.gov. Available online: https://www.frames.gov/catalog/23672 (accessed on 18 January 2026).
39. Jiménez, P.A.; Dudhia, J. On the ability of the WRF model to reproduce the surface wind direction over complex terrain. *J. Appl. Meteorol. Climatol.* **2013**, *52*, 1610–1617. [CrossRef]
40. Brown, M.J.; Nelson, M.A.; Conry, P.T.; Boukhalfa, H.; Brug, W.P.; Rahn, T.A. *EMRTC 2019 Winds in Complex Terrain Campaign*; Technical Report LA-UR-25-24005; Los Alamos National Laboratory: Los Alamos, NM, USA, 2025.
41. Charney, J.J.; Kiefer, M.T.; Zhong, S.; Heilman, W.E.; Nikolic, J.; Bian, X.; Hom, J.L.; Clark, K.L.; Skowronski, N.S.; Gallagher, M.R.; et al. Assessing forest canopy impacts on smoke concentrations using a coupled numerical model. *Atmosphere* **2019**, *10*, 273. [CrossRef]
42. Massman, W.J.; Forthofer, J.; Finney, M.A. An improved canopy wind model for predicting wind adjustment factors and wildland fire behavior. *Can. J. For. Res.* **2017**, *47*, 594–603. [CrossRef]
43. National Weather Service. National Weather Service—Weather.gov. Available online: https://weather.gov (accessed on 18 January 2026).
44. WIFIRE. BurnPro3D | WIFIRE—Wifire.ucsd.edu. Available online: https://burnpro3d.sdsc.edu/index.html (accessed on 18 January 2026).
45. Lang, S.; Alexe, M.; Chantry, M.; Dramsch, J.; Pinault, F.; Raoult, B.; Clare, M.C.; Lessig, C.; Maier-Gerber, M.; Magnusson, L.; et al. AIFS–ECMWF's data-driven forecasting system. *arXiv* **2024**, arXiv:2406.01465.
46. Google. WeatherNext 2—Developers.google.com. Available online: https://developers.google.com/earth-engine/datasets/catalog/projects_gcp-public-data-weathernext_assets_weathernext_2_0_0 (accessed on 18 January 2026).
47. Tomorrow.io. Low-Level Winds and Temperature (Aviation, Premium Layer)—Support.tomorrow.io. Available online: https://support.tomorrow.io/hc/en-us/articles/16452977593620-Low-Level-Winds-and-Temperature-Aviation-Premium-Layer (accessed on 18 January 2026).
48. AccuWeather. AccuWeather for Business Products and Services. Available online: https://business.accuweather.com/products/ (accessed on 15 March 2026).
49. Li, Y.; Tong, D.; Ngan, F.; Cohen, M.; Stein, A.; Kondragunta, S.; Zhang, X.; Ichoku, C.; Hyer, E.; Kahn, R. Ensemble PM2.5 forecasting during the 2018 camp fire event using the HYSPLIT transport and dispersion model. *J. Geophys. Res. Atmos.* **2020**, *125*, e2020JD032768. [CrossRef]
50. Lian, J.; Huang, S.; Shao, J.; Chen, P.; Tang, S.; Lu, Y.; Yu, H. TerraWind: A deep learning-based near-surface winds downscaling model for complex terrain region. *Geophys. Res. Lett.* **2024**, *51*, e2024GL112124. [CrossRef]
51. Jimenez, M.A.; Cuxart, J. A study of the nocturnal flows generated in the north side of the Pyrenees. *Atmos. Res.* **2014**, *145*, 244–254. [CrossRef]
52. Lehner, M.; Whiteman, C.D.; Hoch, S.W.; Crosman, E.T.; Jeglum, M.E.; Cherukuru, N.W.; Calhoun, R.; Adler, B.; Kalthoff, N.; Rotunno, R.; et al. The METCRAX II field experiment: A study of downslope windstorm-type flows in Arizona's Meteor Crater. *Bull. Am. Meteorol. Soc.* **2016**, *97*, 217–235. [CrossRef]
53. Charrondière, C.; Brun, C.; Cohard, J.M.; Sicart, J.E.; Obligado, M.; Biron, R.; Coulaud, C.; Guyard, H. Katabatic winds over steep slopes: Overview of a field experiment designed to investigate slope-normal velocity and near-surface turbulence. *Bound.-Layer Meteorol.* **2022**, *182*, 29–54. [CrossRef]
54. Hoch, S.W.; Thomas, M.L.; Huwald, H.; Lehning, M.; van Schaik, B.J.; Imbert, P.; Rentel, D.S.; Wirth, V. The MatterHEX Experiment–Investigating Atmospheric Flow Patterns in Highly Complex Terrain Related to Banner Cloud Formation. *Bull. Am. Meteorol. Soc.* **2025**, *106*, E1687–E1702. [CrossRef]
55. Office of the Chief. *Gallinas-Las Dispensas Prescribed Fire Declared Wildfire Review*; Technical report; U.S. Forest Service: Washington, DC, USA, 2022.
56. Vrac, M.; Drobinski, P.; Merlo, A.; Herrmann, M.; Lavaysse, C.; Li, L.; Somot, S. Dynamical and statistical downscaling of the French Mediterranean climate: Uncertainty assessment. *Nat. Hazards Earth Syst. Sci.* **2012**, *12*, 2769–2784. [CrossRef]
57. Zorita, E.; Von Storch, H. The analog method as a simple statistical downscaling technique: Comparison with more complicated methods. *J. Clim.* **1999**, *12*, 2474–2489. [CrossRef]
58. Meng, X.; Zhao, H.; Shu, T.; Zhao, J.; Wan, Q. Machine learning-based spatial downscaling and bias-correction framework for high-resolution temperature forecasting. *Appl. Intell.* **2024**, *54*, 8399–8414. [CrossRef]
59. Bouallègue, Z.B.; Cooper, F.; Chantry, M.; Düben, P.; Bechtold, P.; Sandu, I. Statistical modeling of 2-m temperature and 10-m wind speed forecast errors. *Mon. Weather. Rev.* **2023**, *151*, 897–911. [CrossRef]

60. Oh, M.; Lee, J.; Kim, J.Y.; Kim, H.G. Machine learning-based statistical downscaling of wind resource maps using multi-resolution topographical data. *Wind. Energy* **2022**, *25*, 1121–1141. [CrossRef]
61. Dujardin, J.; Lehning, M. Wind-Topo: Downscaling nearsurface wind fields to high-resolution topography in highly complex terrain with deep learning. *Q. J. R. Meteorol. Soc.* **2022**, *148*, 1368–1388. [CrossRef]
62. Kolukula, S.S.; Murty, P.; Baduru, B.; Sharath, D.; PA, F. Downscaling of wind fields on the east coast of India using deep convolutional neural networks and their applications in storm surge computations. *J. Water Clim. Change* **2024**, *15*, 1612–1628. [CrossRef]
63. Lockwood, J.W.; Gori, A.; Gentine, P. A generative super-resolution model for enhancing tropical cyclone wind field intensity and resolution. *J. Geophys. Res. Mach. Learn. Comput.* **2024**, *1*, e2024JH000375. [CrossRef]
64. Peng, W.; Qin, S.; Yang, S.; Wang, J.; Liu, X.; Wang, L.L. Fourier neural operator for real-time simulation of 3D dynamic urban microclimate. *Build. Environ.* **2024**, *248*, 111063. [CrossRef]
65. Lin, C.; Tie, R.; Yi, S.; Zhong, X.; Li, H. Terrain-aware Deep Learning for Wind Energy Applications: From Kilometer-scale Forecasts to Fine Wind Fields. *arXiv* **2025**, arXiv:2505.12732.
66. Lu, Y.; Zhou, X.H.; Xiao, H.; Li, Q. Using machine learning to predict urban canopy flows for land surface modeling. *Geophys. Res. Lett.* **2023**, *50*, e2022GL102313. [CrossRef]
67. Kastner, P.; Dogan, T. A GAN-based surrogate model for instantaneous urban wind flow prediction. *Build. Environ.* **2023**, *242*, 110384. [CrossRef]
68. Shao, X.; Liu, Z.; Zhang, S.; Zhao, Z.; Hu, C. PIGNN-CFD: A physics-informed graph neural network for rapid predicting urban wind field defined on unstructured mesh. *Build. Environ.* **2023**, *232*, 110056. [CrossRef]
69. Jasiewicz, J.; Stepinski, T.F. Geomorphons—A pattern recognition approach to classification and mapping of landforms. *Geomorphology* **2013**, *182*, 147–156. [CrossRef]
70. Cook, N.J. Implications of the OEN mixture model of the mean wind vector for the generation of synthetic timeseries and for the assessment of extremes. *J. Wind. Eng. Ind. Aerodyn.* **2021**, *208*, 104424. [CrossRef]
71. Cook, N.J. Parameterizing the seasonal–diurnal wind climate of Rome: Fiumicino and Ciampino. *Meteorol. Appl.* **2020**, *27*, e1848. [CrossRef]
72. National Laboratory of the Rockies. Wind Integration National Dataset Toolkits | Grid Modernization | NLR—Nrel.gov. Available online: https://www.nrel.gov/grid/wind-toolkit (accessed on 18 January 2026).
73. Vannitsem, S.; Bremnes, J.B.; Demaeyer, J.; Evans, G.R.; Flowerdew, J.; Hemri, S.; Lerch, S.; Roberts, N.; Theis, S.; Atencia, A.; et al. Statistical postprocessing for weather forecasts: Review, challenges, and avenues in a big data world. *Bull. Am. Meteorol. Soc.* **2021**, *102*, E681–E699. [CrossRef]
74. Han, L.; Chen, M.; Chen, K.; Chen, H.; Zhang, Y.; Lu, B.; Song, L.; Qin, R. A deep learning method for bias correction of ECMWF 24–240 h forecasts. *Adv. Atmos. Sci.* **2021**, *38*, 1444–1459. [CrossRef]
75. Pang, C.; Song, T.; Sun, H.; Li, X.; Xu, D. A deep learning method for bias correction of wind field in the South China Sea. *Front. Mar. Sci.* **2025**, *11*, 1429057. [CrossRef]
76. Zhang, W.; Jiang, Y.; Dong, J.; Song, X.; Pang, R.; Guoan, B.; Yu, H. A deep learning method for real-time bias correction of wind field forecasts in the Western North Pacific. *Atmos. Res.* **2023**, *284*, 106586. [CrossRef]
77. Scher, S.; Messori, G. Predicting weather forecast uncertainty with machine learning. *Q. J. R. Meteorol. Soc.* **2018**, *144*, 2830–2841. [CrossRef]
78. Chu, Y.; Li, C.; Wang, Y.; Li, J.; Li, J. A long-term wind speed ensemble forecasting system with weather adapted correction. *Energies* **2016**, *9*, 894. [CrossRef]
79. Zhou, X.; Sun, Y.; Wu, J.; Huang, X. How to systematically develop an effective AI-based bias correction model? *arXiv* **2025**, arXiv:2504.15322. [CrossRef]
80. National Weather Service. Model Analyses and Guidance. Available online: https://mag.ncep.noaa.gov/model-guidance-model-area.php (accessed on 1 February 2026).
81. Department of Defense. WFSI Data Portal. Available online: https://wfsi-data.org/ (accessed on 1 February 2026).
82. Lam, R.; Sanchez-Gonzalez, A.; Willson, M.; Wirnsberger, P.; Fortunato, M.; Alet, F.; Ravuri, S.; Ewalds, T.; Eaton-Rosen, Z.; Hu, W.; et al. Learning skillful medium-range global weather forecasting. *Nature* **2023**, *383*, 1416–1421. [CrossRef]
83. National Weather Service. Fire Weather—Weather.gov. Available online: https://www.weather.gov/abq/forecasts-fireweather (accessed on 23 September 2025).
84. Li, Z.; Kovachki, N.; Azizzadenesheli, K.; Liu, B.; Bhattacharya, K.; Stuart, A.; Anandkumar, A. Fourier neural operator for parametric partial differential equations. *arXiv* **2020**, arXiv:2010.08895.
85. Giral, F.; Manzano, Á.; Gómez, I.; Koumoutsakos, P.; Clainche, S.L. Generative Urban Flow Modeling: From Geometry to Airflow with Graph Diffusion. *arXiv* **2025**, arXiv:2512.14725.

86. Kashinath, K.; Mustafa, M.; Albert, A.; Wu, J.; Jiang, C.; Esmaeilzadeh, S.; Azizzadenesheli, K.; Wang, R.; Chattopadhyay, A.; Singh, A.; et al. Physics-informed machine learning: Case studies for weather and climate modelling. *Philos. Trans. R. Soc.* **2021**, *379*, 20200093. [CrossRef]
87. Barwey, S.; Pal, P.; Patel, S.; Balin, R.; Lusch, B.; Vishwanath, V.; Maulik, R.; Balakrishnan, R. Mesh-based super-resolution of fluid flows with multiscale graph neural networks. *Comput. Methods Appl. Mech. Eng.* **2025**, *443*, 118072. [CrossRef]